NMRlipids IV: Headgroup & glycerol backbone structures, and cation binding in bilayers with PS lipids

O. H. Samuli Ollila[1, 2, *]

[1]*Institute of Organic Chemistry and Biochemistry, Academy of Sciences of the Czech Republic, Prague 6, Czech Republic*
[2]*Institute of Biotechnology, University of Helsinki*

(Dated: January 4, 2018)

Primarily measured but also simulated NMR order parameters will be collected also for other than phophatidylcholine (these are discussed in NMRlipids I) headgroup. The information will be used to understand structural differences between different lipid molecules in bilayers.

INTRODUCTION

In NMRlipids I and II project we were looking for a MD model which would correctly reproduce headgroup and glycerol backbone structures and cation binding for PC lipid bilayers [1, 2]. Here we extend the same goal for lipids with negatively charged PS headgroup. Chemical structure of PS headgroup together with other common biological lipids is shown in Fig. 1.

Glycerol backbone and headgroup structure and behaviour are similar in model membranes and in bacteria [3–5].

METHODS

Solid state NMR experiments

The experimental protocol is the same used in Ref. 6.

Molecular dynamics simulations

Molecular dynamics simulation data was collected with Open Collaboration method. The simulated systems are listed in Table I. The simulation details are in SI or in references in the table.

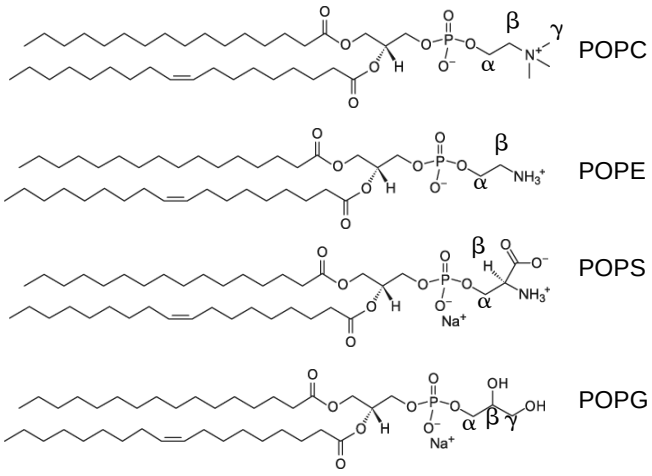

FIG. 1: Chemical structures and labels for the headgroup carbons.

RESULTS AND DISCUSSION

Headgroup and glycerol backbone order parameters measured from POPS lipid bilayer

Figs. 2 and 3 summarize the experimental NMR results for POPS bilayer sample.

The headgroup and glycerol backbone order parameters of POPS measured in this work are compared to the literature values of DOPS [29] and POPC [30] in Fig. 4. Our results for POPS are in good agreement with the previously reported values for DOPS measured with ^{2}H NMR. Significant differences are observed between PC and PS lipids, especially at the headgroup region. Previous discussions in the literature have concluded that glycerol backbone structure is largely similar in PC, PE, PG and PS lipids [3]. The headgroup region was found to be similar in PC, PE and PG lipid (assuming that the signs of PE and PG order parameters are the same as in PC), while the PS headgroup was suggested to be more rigid [31, 32]. The detailed structural differences between the headgroups is, however, not known.

Headgroup and glycerol backbone in simulations of PS lipid bilayers

The headgroup order parameters of DOPS and POPS bilayers from different simulation models are compared with the experimental data in Fig. 5. In line with the previous study for PC lipids [1], the glycerol backbone order parameters in CHARMM36 and Berger force fields roughly agree with the experimental data, but significant discrepancies are observed for Slipids and CKP models. The glycerol backbone structures from CHARMM36 and Slipids simulations visualized in Fig. 7 reveal the missing structures in Slipids model, which probably lead to the incorrect order parameters. For the headgroup α and β carbon order parameters of PS lipids, the tested models perform less well than for PC headgroup in previous study [1]. None of the tested models give a satisfactory agreement with experiments for the headgroup order paramaters of

TABLE I: List of MD simulations. The salt concentrations calculated as [salt]=$N_c \times$[water] / N_w, where [water] = 55.5 M. CKP1 referes to the version with Berger/chiu NH3 charges compatible with Berger and CKP2 to the version with more Gromos compatible version.

lipid/counter-ions	force field for lipids / ions	NaCl (mM)	$CaCl_2$ (mM)	[a]N_l	[b]N_w	[c]N_c	[d]T (K)	[e]t_{sim}(ns)	[f]t_{anal} (ns)	[g]files
DPPE	Slipids [7]	0	0	288	9386	0	336	200	100	[8]
DOPS/Na^+	CHARMM36 [**?**] **1.**	0	0	128	4480	0	303	500	100	[9]
DOPS/Na^+	CHARMM36ua [**?**] **2.**	0	0	128	4480	0	303	500	100	[10]
DOPS/Na^+	Slipids [11]	0	0	128	4480	0	303	500	100	[12]
DOPS/Na^+	Slipids [11]	0	0	288	11232	0	303	200	100	[13]
DOPS/Na^+	Berger [14]	0	0	128	4480	0	303	500	100	[15]
DOPS/Na^+	GROMOS-CKP1 [**?**] **3.**	0	0	128	4480	0	303	500	100	[16]
DOPS/Na^+	GROMOS-CKP2 [**?**] **4.**	0	0	128	4480	0	303	500	100	[17]
POPS/Na^+	CHARMM36 [**?**] **5.**	0	0	128	4480	0	298	500	100	[18]
POPS/Na^+	CHARMM36ua [**?**] **6.**	0	0	128	4480	0	298	500	100	[19]
POPS/Na^+	Slipids [11]	0	0	128	4480	0	298	500	100	[20]
POPS/Na^+	Berger [**?**]	0	0	128	4480	0	298	500	100	[21]
POPS/Na^+	MacRog [22]	0	0	128	5120	0	298	200	? **7.**	[23]
POPS/Na^+	GROMOS-CKP1 [**?**] **8.**	0	0	128	4480	0	298	500	100	[24]
POPS/Na^+	GROMOS-CKP2 [**?**] **9.**	0	0	128	4480	0	298	500	100	[25]
POPC:POPS (5:1)/K^+	CHARMM36 [26**?**] **10.**	0	0	110:22	4935	0	298	100	100 **11.**	[27]

[a]Number of lipid molecules with largest mole fraction
[b]Number of water molecules
[c]Number of additional cations
[d]Simulation temperature
[e]Total simulation time
[f]Time used for analysis
[g]Reference for simulation files

PS lipids. Based on the subjective ranking shown in Fig. 6, the CHARMM36 is the best performing model for both lipids. However, the total deviation from the experiments for the PS lipids is significantly higher for PS lipids (8) than for PC (3) [1]. Therefore the interpretation of structural differences between PC and PS lipids from current MD simulation models is very challenging.

19.Dihedral angle distribtions in Fig. 13 should be analyzed from different models and included in the discussion. Maybe also figures similar to 7.

Headgroup structure in PS and PC mixtures

Lipid mixtures containing PC and PS lipids are present in biological systems. Also the Ca2+ binding affinity to bilayers containing PS lipids is measured from mixtures with PC, because pure PS bilayers exhibit instant transition to the ordered phase with the addition of the ions. Therefore, the characterization of mutual interactions between PC and PS lipid headgroups is necessary in order to understand PS lipids in biological environments.

Fig. 8 shows the headgroup order parameters of POPC and POPS lipids in mixtures with various mole fractions from simulations and experiments [4, 33]. The headgroup order parameters of POPC increase with the increasing amount of negatively charged POPS, as expected from the the electrometer concept [34]. Notably, the concept seems to be generally valid, at least qualitatively, also for other lipid mixed with PC lipids; the PC lipid headgroup order parameters increase when mixed with negatively charged lipids (PS, PI, CL, PA and PG) and remains almost unchaged when mixed with neutral lipids (PE and SM) [4] or cholesterol [30]. This is, however, not reproduced in the simulation data in Fig. 8. The order parameter for β-carbon of POPC decreases and almost negligible increase is seen in α order parameter with the addition of PS lipid in CHARMM36 simulation. This may indicate incorrect interactions between PC and PS headgroups in simulations. On the other hand, the previously reported overestimated ion binding affinity may also play a role, as the amount of counterions is increasing with PS. **20.Data from other force fields to be collected before discussion can be finalized.**

Also the headgroup order parameters of POPS mixed with varying amounts of POPC from simulations and experiments [33, 36] are shown in Fig. 8. The β-carbon order parameter of POPS slightly decreases and positive order parameter of α-carbon slightly increases with increasing amount of PS lipids. This may indicate increasing order of the headgroup. It should be, however, noted that the experimental data for pure POPS and POPC/POPS mixture come from different experimental sets, 13C NMR in this work and 2H NMR from Ref. 33, respectively. Therefore the accuracy of the order parameter change is not as high as typically in the mea-

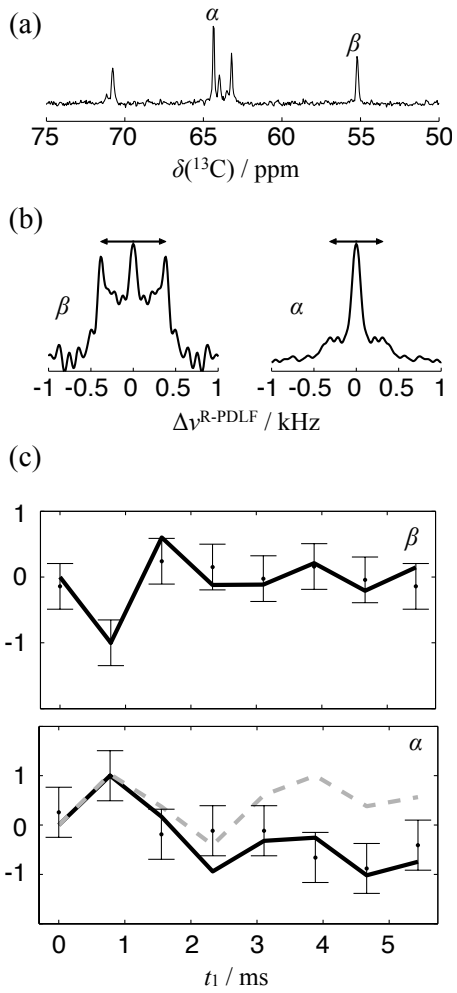

FIG. 2: (a) The headgroup region of the INEPT spectrum where alpha and beta are identified. (b) The R-PDLF slices for alpha and beta showing one single splitting for beta (which gives an order parameter equal to 0.12), and for alpha a superposition of a large splitting (order parameter equal to 0.09) and a very small splitting which cannot resolved with the available resolution. (c) Points with error bars are the experimental SDROSS data. The thick lines are SIMPSON simulations. The S-DROSS slice for beta clearly shows that the order parameter is negative, which is confirmed by SIMPSON simulations using the order parameter value of -0.12. The S-DROSS slice for alpha suggests that the higher order parameter is positive and the deviation towards negative values in the longer t1 times suggests that the smaller order parameter is negative. This is confirmed by SIMPSON simulation using value of 0.09 for the larger alpha order parameter and the value of -0.02 for smaller (black curve). The value for the smaller alpha order parameter for SIMPSON calculation was taken from Fig 3 in Ref. 28, because resolution in 13C NMR experiments was nor high enough to determine numerical value for this. The S-DROSS curve from SIMPSON simulation with positive value for the smaller order parameter gave did not agree with experiments (dashed grey), confirming the interpretation that the smaller order parameter is negative.

12.Maybe we should combine this with 3

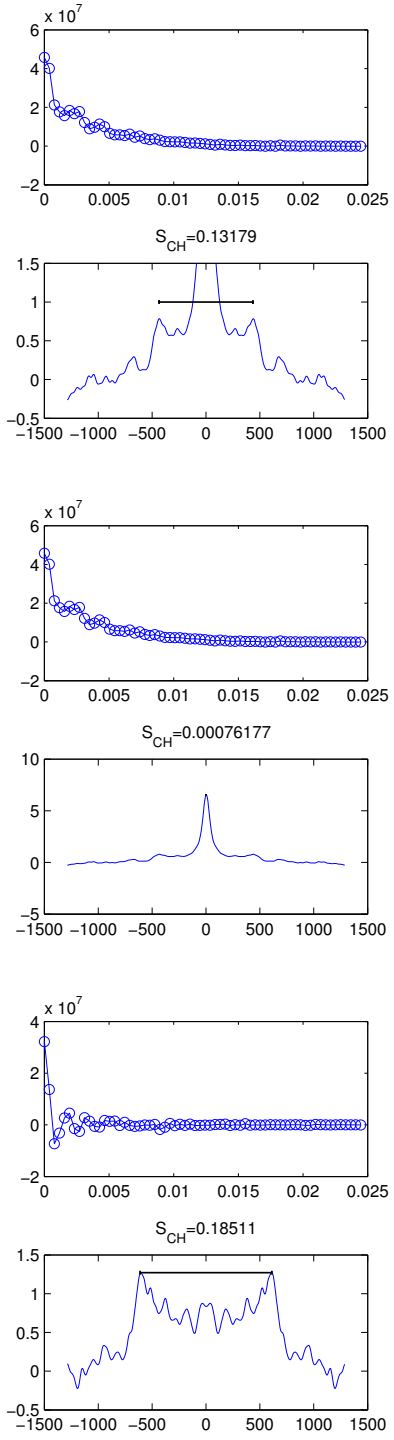

FIG. 3: R-PDFL slices for gycerol backbone carbons.

13.We need nicer figure for this data. Maybe combine with 2

14.What are the top figures actually?

surements of order parameter changes, see discussion about qualitative and quantitative accuracy in Ref. 35. The changes of PS headgroup order parameters are not reproduced by the tested simulation models. The β-carbon order parameter in-

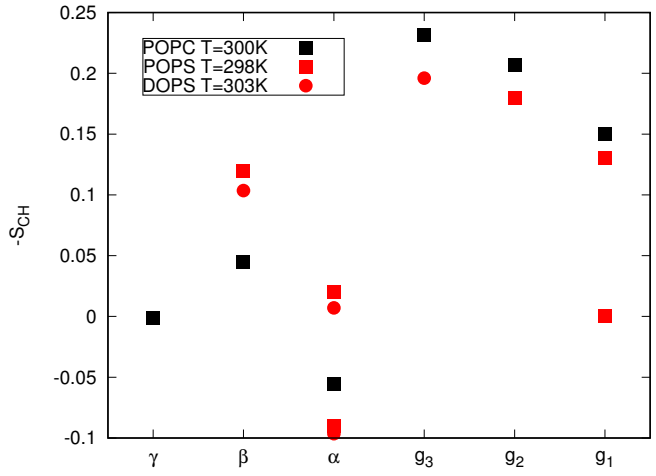

FIG. 4: Headgroup and glycerol backbone order parameters of POPS measured in this work compared with values for DOPS (^{2}H NMR, 0.1M of NaCl) [29] and POPC (^{13}C NMR) [30] from literature. Signs for PS order parameters as measured in this work and signs for PC as measured in Refs [6**?**].

crease with increasing amount of PS in CHARMM36 and MacRog simulations in contrast to the experimental data. The smaller α-carbon order parameter increase in both simulation models with increasing amount of PS, while it is almost unchanged in experiments. The larger α-carbon order parameter increase in MacRog and decrease in CHARMM36 with increasing amount of PS, both model exhibiting a poor agreement with experiments. Signifincant improvement in the MD simulation models are needed to interpret the PS headgroup structures and mutual interactions with PC lipids.

Ca^{2+} binding affinity in bilayers with negatively charged PS lipids

PC lipid headgroup order parameters can used to measure ion binding affinity, because their magnitude is proportional to the amount of bound charge in bilayer [2, 34]. The molecular electrometer concept can be used also for bilayers containing PC lipids mixed with charged lipids [33, 36, 37]. This is demonstrated in Fig. 9, showing the changes of PC headgroup order parameters as a function of $CaCl_2$ concentration in the presence of different amounts of negatively charged PS or PG lipids. The decrease of order parameters with $CaCl_2$ is more pronounced for systems with more negatively charged lipids.Order parameters reach the values of pure PC bilayer close to $CaCl_2$ concentrations of $\sim$ 50-300mM. At this point the Ca2+ binding presumably fully cancels the charge from negative lipids and overcharging occurs above these concenterations. The interpretation of this data and some other results has been that [5]

> *"(i) Ca^{2+} binds to neutral lipids (phosphatidylcholine, phosphatidylethanolamine) and nega-*

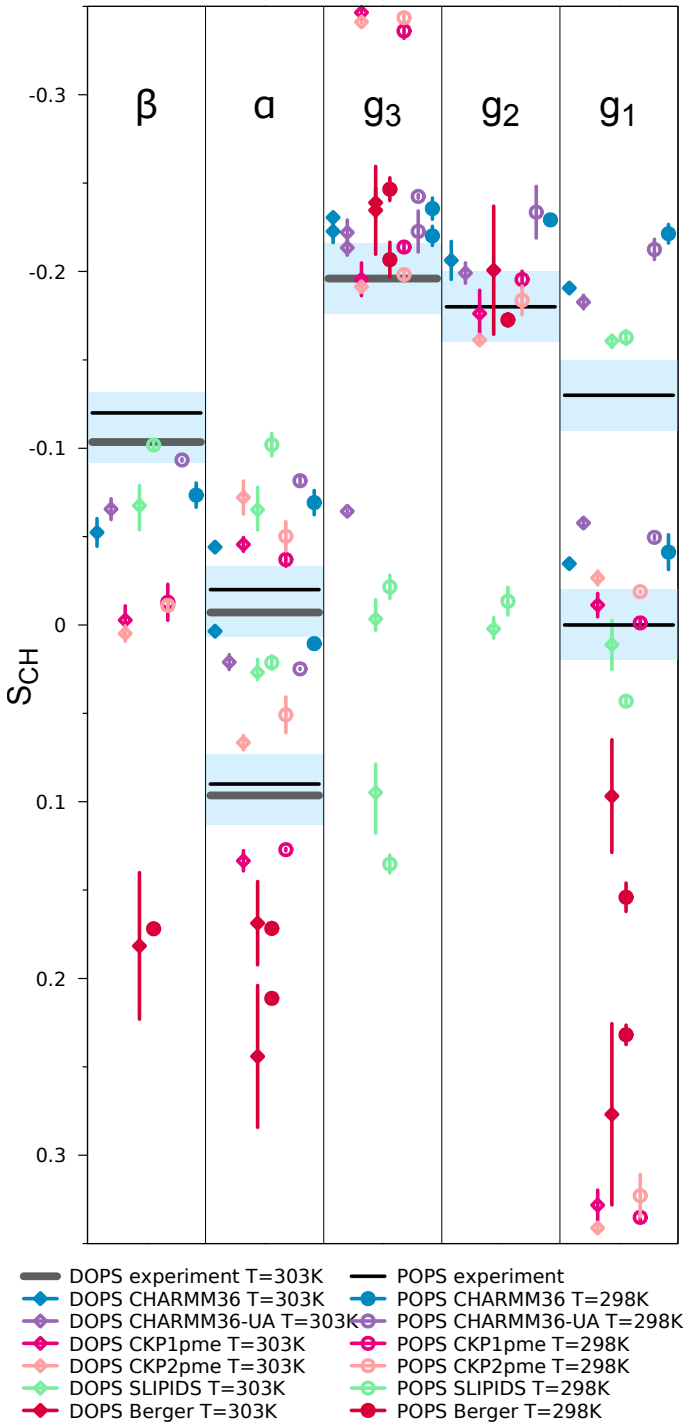

FIG. 5: Order parameters for PS headgroup and glycerol backbone from simulations with different models and experiments without $CaCl_2$ Experimental data from [29] contains 0.1M of NaCl. Signs are taken from experiments for POPS described in Supplementary Information. The vertical bars shown for the computational values are not error bars, but demonstrate that for these systems we had at least two data sets; the ends of the bars mark the extreme values from the sets, and the dot marks their measurement-time-weighted average.

15.Check and report all the counterions. There may be some simulation data sets with both Na+ and K+ ions? 16.CHARMM36-UA point for alpha in wrong place? 17.MacRog POPS data missing. The equilibration yet to be checked, thought. 18.In table I: "CKP1 referes to the version with Berger/chiu NH3 charges compatible with Berger and CKP2 to the version with more Gromos compatible version." Is this correct also in this figure?

	β	α	g_3	g_2	g_1	Σ
CHARMM 36	M	M F	M	M	**M** F	8
CHARMM 36-UA	M	M	M	M	**M** F	8
GROMOS-CKP1	**M**	M **F**	**M F**		**M F**	14
GROMOS-CKP2	**M**	M F	**M F**		**M F**	14
Slipid	M	**M**	**M F**	**M**	M **F**	14
Berger	**M**	**M F**	M F	M	**M** F	15

FIG. 6: Rough subjective ranking of force fields based on Figure 5. Here M indicates a magnitude problem, F a forking problem; letter size increases with problem severity. Color scheme: within experimental error (dark green), almost within experimental error (light green), clear deviation from experiments (light red), and major deviation from experiments (dark red). The Σ-column shows the total deviation of the force field, when individual carbons are given weights of 0 (matches experiment), 1, 2, and 4 (major deviation). For full details of the assessment, see Supplementary Information.

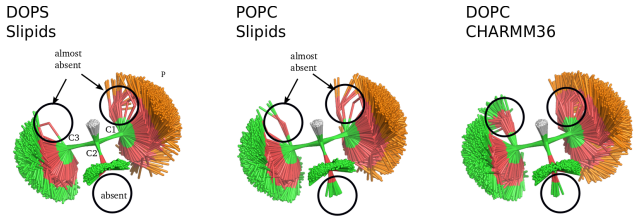

FIG. 7: Snapshots overlayed from different simulations for glycerol backbone region by Pavel Buslaev.

tively charged lipids (phosphatidylglycerol) with approximately the same binding constant of K = 10-20 M^{-1};
(ii) the free Ca^{2+} concentration at the membrane interface is distinctly enhanced if the membrane carries a negative surface charge, either due to protein or to lipid;
(iii) increased inter-facial Ca^{2+} also means increased amounts of bound Ca^{2+} at neutral and charged lipids;
(iv) the actual binding step can be described by a Langmuir adsorption isotherm with a 1 lipid:1 Ca^{2+} stoichiometry, provided the interfacial concentration C_M, is used to describe the chemical binding equilibrium."

Before using headgroup order parameters to compare ion binding affinity between simulations and experiments, the response of the order parameters to bound charge has to be quantified. The response of headgroup order parameters to the fixed amount of cationic surfactants in POPC bilayer is compared between simulations and experiments [38] In Fig. 10. The figure shows that the order parameters are too sensitive to bound charge in Lipid14 model, while CHARMM36 is in better agreement with experiments. This has to be taken into account when analysin the binding affinities.

23.When we have more data for Ca binding to PS containing bilayers, the discussion will be updated and PG results moved to other manuscript. Comparison of Ca2+ binding in PG between CHARMM36 simulations and experiments [36] is shown in Fig. 11. The decrease of α order parameter is in agreement with experiments, while decerase of β order parameter is overestimated. The result is very similar to the results with PC in NMRlipids II publication [2]. It should be, however, noted that the β-order parameters are not actually measured for PG, but they are calculated from empirical relation $\Delta S_\beta = 0.43\Delta S_\alpha$ [39]. Anyway, the data presented in NMRlipids II project and in Fig. 11 together suggest that Calcium binding is similarly overestimated by CHARMM36 model in pure POPC bilayers and mixtures with POPG. The good agreement of α carbon would be explained by too weak dependence of its order parameter of bound charge

Also dependence of β-carbon of PG on $CaCl_2$ concentration is compared with experiments [36] in Fig. **??**. Absolute value of the order parameter is too large without ions, but rapid decrease due to addition of $CaCl_2$ is observed in agreement with experiments for systems with 1:1 mixture of POPC and POPG. In addition, absolute value in systems with $CaCl_2$ is in agreement with experiments. However, system with 4:1 mixture of POPC and POPG behaves differently, but experimental data is not available for comparison for this mixture.

24.More simulation data for systems with negatively charged lipids and $CaCl_2$ to be collected

Also the experimental order parameters for PS and PG headgroups as a function of $CaCl_2$ concentration are shown in Fig. **??**. **25.These should be compared to simulations for potential structural interpretation of the changes.**

CONCLUSIONS

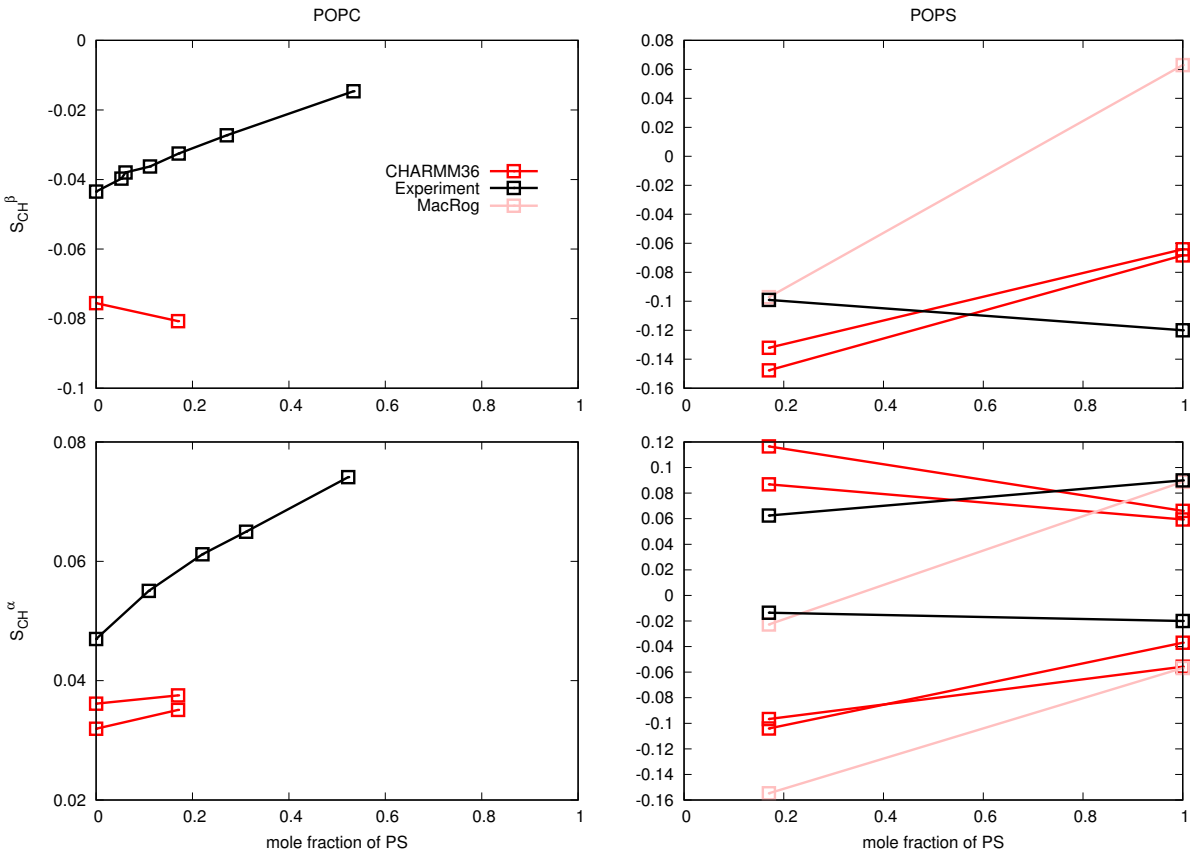

FIG. 8: Headgroup order parameters from PC:PS mixtures from different simulation models and experiments. Left panel shows the PC headgroup order parameters (experimental results from Ref. 4, signs are determined as discussed in [1, 35]). Rigth panel shows PS headgroup order parameters (experimental result for pure POPS measured in this work at 298K, experimental result for mixture from Ref. 33 at 298K). Counterions in expriments are sodium, while potassium is used in simulations. Using sodium in simulations do not have a significant effect.

21.Simulation of CHARMM36 at 298K should be maybe rerun with Gromacs 5.

22.We need results also from other than CHARMM36 force field.

SUPPLEMENTARY INFORMATION

Simulated systems

PC lipid headgroup response to different mixtures in experiments

As shown in Fig. 12, order parameters of PC headgroup behave in various lipid mixtures as expected from the electrometer concept [4, 34], i.e., order parameters increase when anionic lipids are mixed with PC and decrease with cationic surfactants. The changes with the addition of neutral lipids is significantly smaller.

Dihedrals

Details of the rough subjective force field ranking (Fig. 6)

The assessment was based fully on the Fig. 5. First, for each carbon (the columns in Fig. 5) in each force field (the rows), we looked separately at deviations in magnitude and forking.

Magnitude deviations, i.e., how close to the experimentally obtained C–H order parameters (OPs) the force-field-produced OPs were. For each carbon, the following 5-step scale was used:

0 ( ): More than half of all the calculated OPs (that is, of all different hydrogens in all different lipids) were within the *subjective sweet spots* (SSP, blue-shaded areas in Fig. 5).

1 (ᴍ): All the calculated OPs were < 0.03 units away from the SSP.

2 (M): All the calculated OPs were < 0.05 units away from the SSP.

3 (M): All the calculated OPs were < 0.10 units away

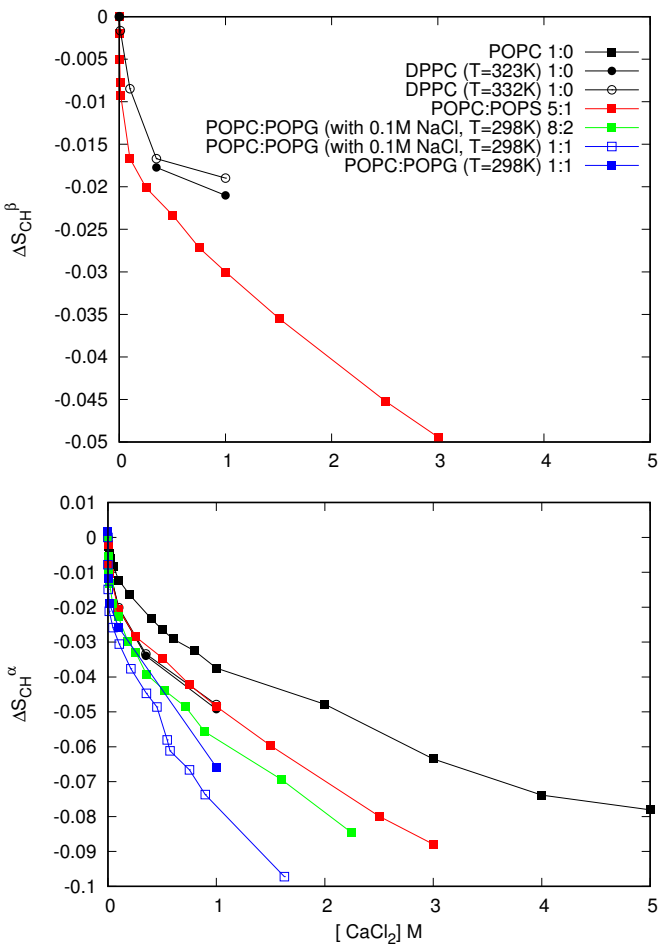

FIG. 9: The change of PC headgroup order parameters in the presence of different amount of negatively charged lipids respect to the values without added $CaCl_2$. The original data is the same as in Fig. **??**.

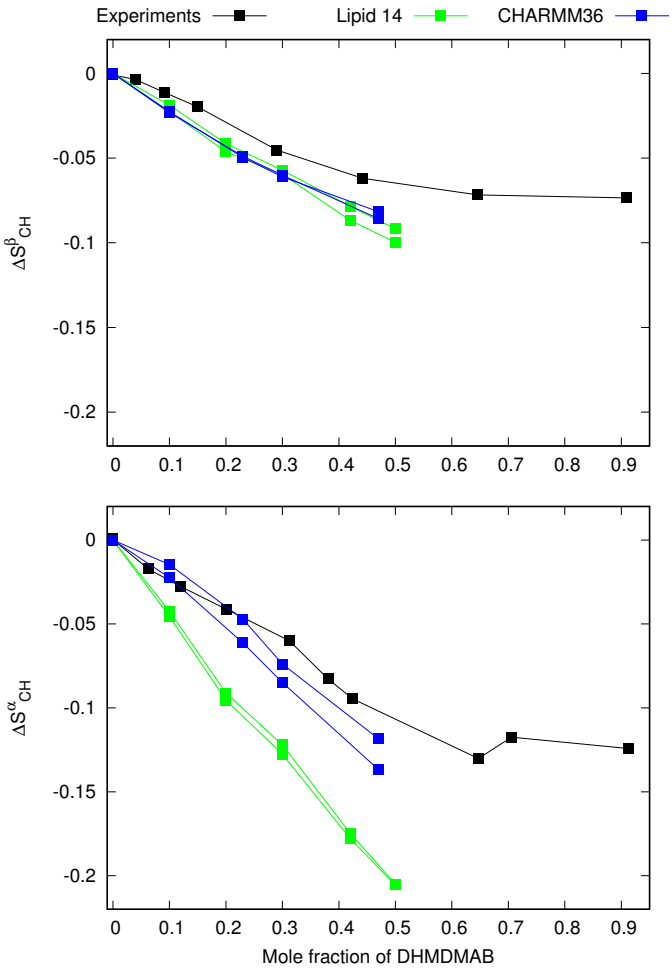

FIG. 10: The response of headgroup order parameters to the fixed amount of cationic surfactants in POPC bilayer is compared between simulations and experiments [38].

from the SSP.

4 (M): Some of the calculated OPs were > 0.10 units away from the SSP.

Forking deviations, i.e., how well the difference in order parameters of two hydrogens attached to a given carbon matched that obtained experimentally. Note that this is not relevant for β and g_2, which have only one hydrogen. For the α carbon, for which a considerable forking of 0.105 is experimentally seen, the following 5-step scale was used:

0 ( ): The distance D between the dots (that mark the measurement-time-weighted averages in Fig. 5) was $0.08 < D < 0.13$ units for all the calculated OPs (that is, for all different lipids).

1 (F): $(0.06 < D < 0.08)$ OR $(0.13 < D < 0.15)$.

2 (F): $(0.04 < D < 0.06)$ OR $(0.15 < D < 0.17)$.

3 (F): $(0.02 < D < 0.04)$ OR $(0.17 < D < 0.19)$.

4 (F): $(D < 0.02)$ OR $(0.19 < D)$.

For the g_3 carbon, for which no forking is indicated by experiments, the following 5-step scale was used:

0 ( ): $D < 0.02$.

1 (F): $0.02 < D < 0.04$.

2 (F): $0.04 < D < 0.06$.

3 (F): $0.06 < D < 0.08$.

4 (F): $0.08 < D$.

For the g_1 carbon, for which a considerable forking of 0.13 is experimentally seen, the following 5-step scale was used:

0 ( ): $0.11 < D < 0.15$.

1 (F): $(0.09 < D < 0.11)$ OR $(0.15 < D < 0.17)$.

2 (F): $(0.07 < D < 0.09)$ OR $(0.17 < D < 0.19)$.

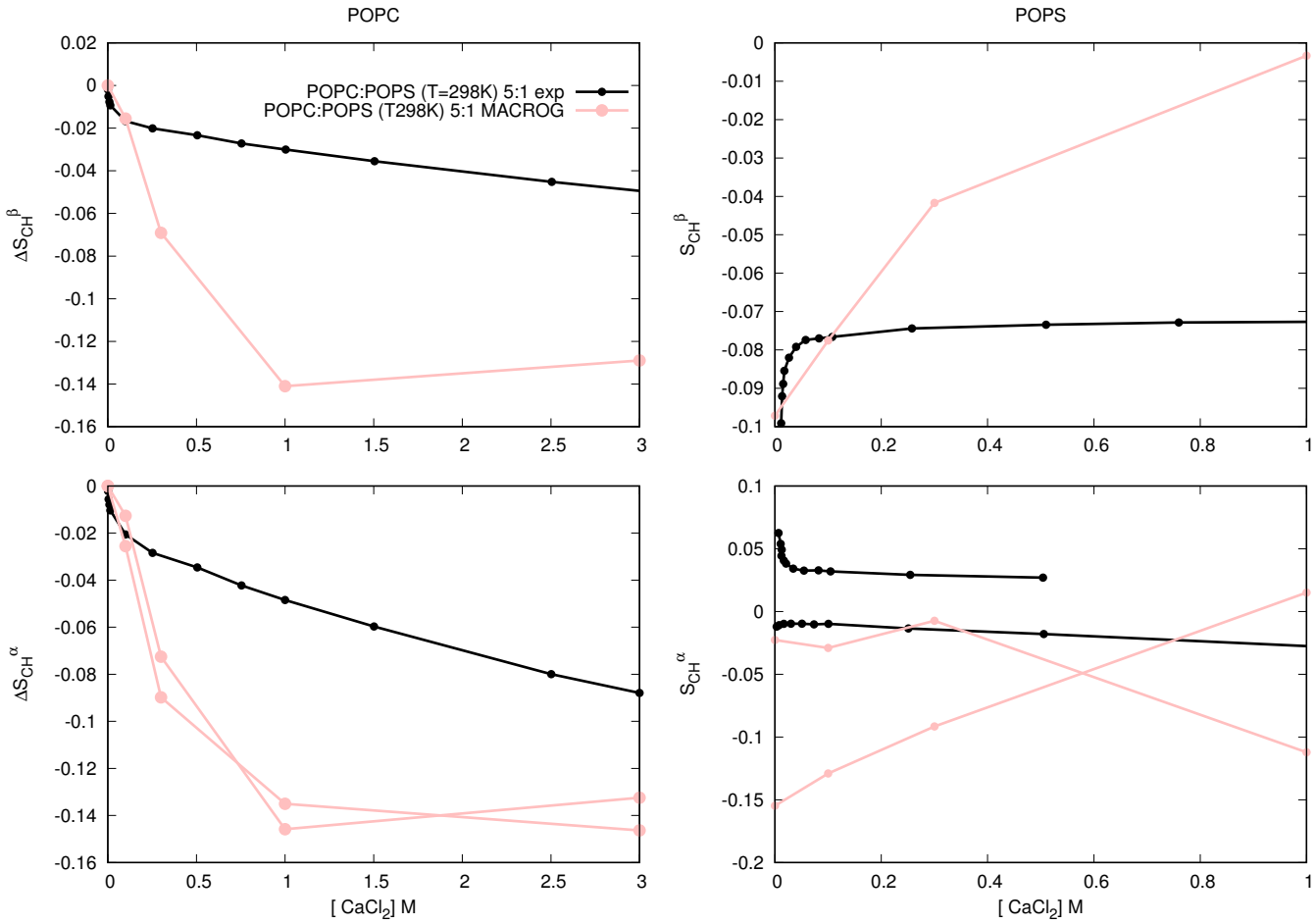

FIG. 11: PG order parameters as a function $CaCl_2$ concentration from experiments [36] and CHARMM36 simulations. Note that beta order parameter is calculated from empirical relation $\Delta S_\beta = 0.43 \Delta S_\alpha$ [39], not actually measured.

3 (F): $(0.05 < D < 0.07)$ OR $(0.19 < D < 0.21)$.

4 (F): $(D < 0.05)$ OR $(0.21 < D)$.

Based on these assessments of magnitude and forking deviations, each carbon was then assigned to one of the following groups: "within experimental error" (magnitude and forking deviations both on step 0 of the scales described above), "almost within experimental error" (sum of the magnitude and forking deviation steps 1 or 2), "clear deviation from experiments" (sum of magnitude and forking deviation steps from 3 to 5), and "major deviation from experiments" (sum of magnitude and forking deviation steps from 6 to 8). These groups are indicated by colors in Fig. 4. (Note that for β and g_2, for which there can be no forking, the corresponding group assigment limits were: 0, 1, 2, and 3.)

Finally, the total ability of the force field to describe the headgroup and glycerol structure was estimated. To this end, the groups were given the following weights: 0 (within experimental error), 1 (almost within experimental error), 2 (clear deviation from experiments), 4 (major deviation from experiments), and the weights of the five carbons were summed up. The sum, given in the Σ-column of Fig. 5, was then used to (roughly and subjectively, as should be clear from the above description) rank the force fields.

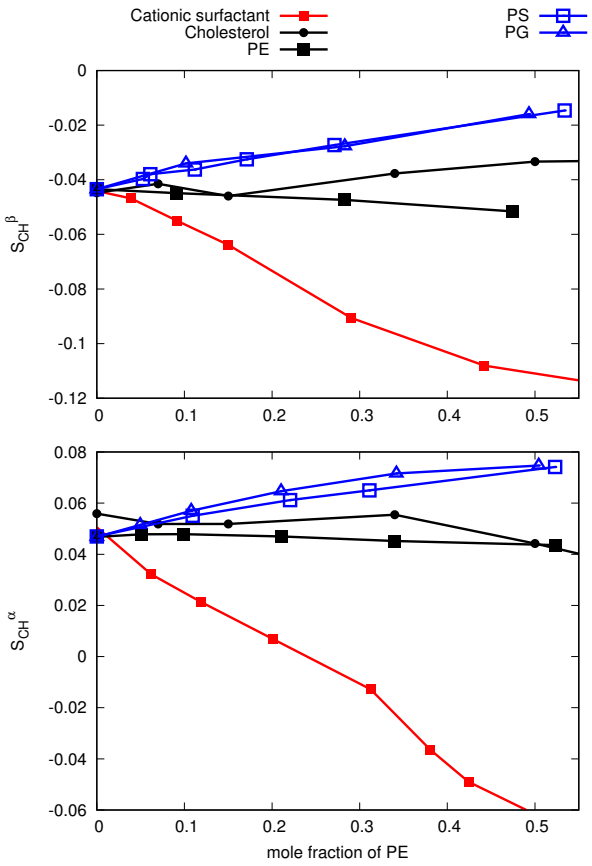

FIG. 12: PC headgroup order parameters from experiments of mixtures with PE, PS, PG and cholesterol [4, 30, 38]. Signs are determined as discussed in [1, 35].

* samuli.ollila@helsinki.fi

[1] A. Botan, F. Favela-Rosales, P. F. J. Fuchs, M. Javanainen, M. Kanduč, W. Kulig, A. Lamberg, C. Loison, A. Lyubartsev, M. S. Miettinen, et al., J. Phys. Chem. B **119**, 15075 (2015).

[2] A. Catte, M. Girych, M. Javanainen, C. Loison, J. Melcr, M. S. Miettinen, L. Monticelli, J. Maatta, V. S. Oganesyan, O. H. S. Ollila, et al., Phys. Chem. Chem. Phys. **18**, 32560 (2016).

[3] H. U. Gally, G. Pluschke, P. Overath, and J. Seelig, Biochemistry **20**, 1826 (1981).

[4] P. Scherer and J. Seelig, EMBO J. **6** (1987).

[5] J. Seelig, Cell Biology International Reports **14**, 353 (1990), ISSN 0309-1651, URL http://www.sciencedirect.com/science/article/pii/030916519091204H.

[6] T. M. Ferreira, R. Sood, R. Bärenwald, G. Carlström, D. Topgaard, K. Saalwächter, P. K. J. Kinnunen, and O. H. S. Ollila, Langmuir **32**, 6524 (2016).

[7] J. P. M. Jämbeck and A. P. Lyubartsev, J. Chem. Theory Comput. **8**, 2938 (2012).

[8] F. Favela-Rosales, *MD simulation trajectory of a fully hydrated DPPE bilayer: SLIPIDS, Gromacs 5.0.4. 2017.* (2017), URL https://doi.org/10.5281/zenodo.495247.

[9] T. Piggot, *CHARMM36 DOPS simulations (versions 1 and 2) 303 K 1.0 nm LJ switching* (2017), URL https://doi.org/10.5281/zenodo.1129411.

[10] T. Piggot, *CHARMM36-UA DOPS simulations (versions 1 and 2) 303 K 1.0 nm LJ switching* (2017), URL https://doi.org/10.5281/zenodo.1129456.

[11] J. P. M. Jämbeck and A. P. Lyubartsev, Phys. Chem. Chem. Phys. **15**, 4677 (2013).

[12] T. Piggot, *Slipids DOPS simulations (versions 1 and 2) 303 K 1.0 nm cut-off with LJ-PME* (2017), URL https://doi.org/10.5281/zenodo.1129439.

[13] F. Favela-Rosales, *MD simulation trajectory of a fully hydrated DOPS bilayer: SLIPIDS, Gromacs 5.0.4. 2017.* (2017), URL https://doi.org/10.5281/zenodo.495510.

[14] P. Mukhopadhyay, L. Monticelli, and D. P. Tieleman, Biophysical Journal **86**, 1601 (2004).

[15] T. Piggot, *Berger DOPS simulations (versions 1 and 2) 303 K 1.0 nm cut-off* (2017), URL https://doi.org/10.5281/zenodo.1129419.

[16] T. Piggot, *GROMOS-CKP DOPS simulations (versions 1 and 2) 303 K with Berger/Chiu NH3 charges and PME* (2017), URL https://doi.org/10.5281/zenodo.1129429.

[17] T. Piggot, *GROMOS-CKP DOPS simulations (versions 1 and 2) 303 K with GROMOS NH3 charges and PME* (2017), URL https://doi.org/10.5281/zenodo.1129447.

[18] T. Piggot, *CHARMM36 POPS simulations (versions 1 and 2) 298 K 1.0 nm LJ switching* (2017), URL https://doi.org/10.5281/zenodo.1129415.

[19] T. Piggot, *CHARMM36-UA POPS simulations (versions 1 and 2) 298 K 1.0 nm LJ switching* (2017), URL https://doi.org/10.5281/zenodo.1129458.

[20] T. Piggot, *Slipids POPS simulations (versions 1 and 2) 298 K 1.0 nm cut-off with LJ-PME* (2017), URL https://doi.org/10.5281/zenodo.1129441.

[21] T. Piggot, *Berger POPS simulations (versions 1 and 2) 298 K 1.0 nm cut-off* (2017), URL https://doi.org/10.5281/zenodo.1129425.

[22] A. Maciejewski, M. Pasenkiewicz-Gierula, O. Cramariuc, I. Vattulainen, and T. Róg, J. Phys. Chem. B **118**, 4571 (2014).

[23] M. Javanainen, *Simulation of a pops bilayer* (2017), URL https://doi.org/10.5281/zenodo.1120287.

[24] T. Piggot, *GROMOS-CKP POPS simulations (versions 1 and 2) 298 K with Berger/Chiu NH3 charges and PME* (2017), URL https://doi.org/10.5281/zenodo.1129431.

[25] T. Piggot, *GROMOS-CKP POPS simulations (versions 1 and 2) 298 K with GROMOS NH3 charges and PME* (2017), URL https://doi.org/10.5281/zenodo.1129435.

[26] J. B. Klauda, R. M. Venable, J. A. Freites, J. W. O'Connor, D. J. Tobias, C. Mondragon-Ramirez, I. Vorobyov, A. D. MacKerell Jr, and R. W. Pastor, J. Phys. Chem. B **114**, 7830 (2010).

[27] O. H. S. Ollila, *POPS+83%popc lipid bilayer simulation at T298K ran CHARMM_GUI force field and Gromacs* (2017), URL https://doi.org/10.5281/zenodo.1011104.

[28] M. Roux and M. Bloom, Biophys. J. **60**, 38 (1991).

[29] J. L. Browning and J. Seelig, Biochemistry **19**, 1262 (1980).

[30] T. M. Ferreira, F. Coreta-Gomes, O. H. S. Ollila, M. J. Moreno, W. L. C. Vaz, and D. Topgaard, Phys. Chem. Chem. Phys. **15**, 1976 (2013).

[31] R. Wohlgemuth, N. Waespe-Sarcevic, and J. Seelig, Biochemistry **19**, 3315 (1980).

[32] G. Büldt and R. Wohlgemuth, The Journal of Membrane Biology **58**, 81 (1981), ISSN 1432-1424, URL http://dx.doi.org/10.1007/BF01870972.

[33] M. Roux and M. Bloom, Biochemistry **29**, 7077 (1990).

[34] J. Seelig, P. M. MacDonald, and P. G. Scherer, Biochemistry **26**, 7535 (1987).

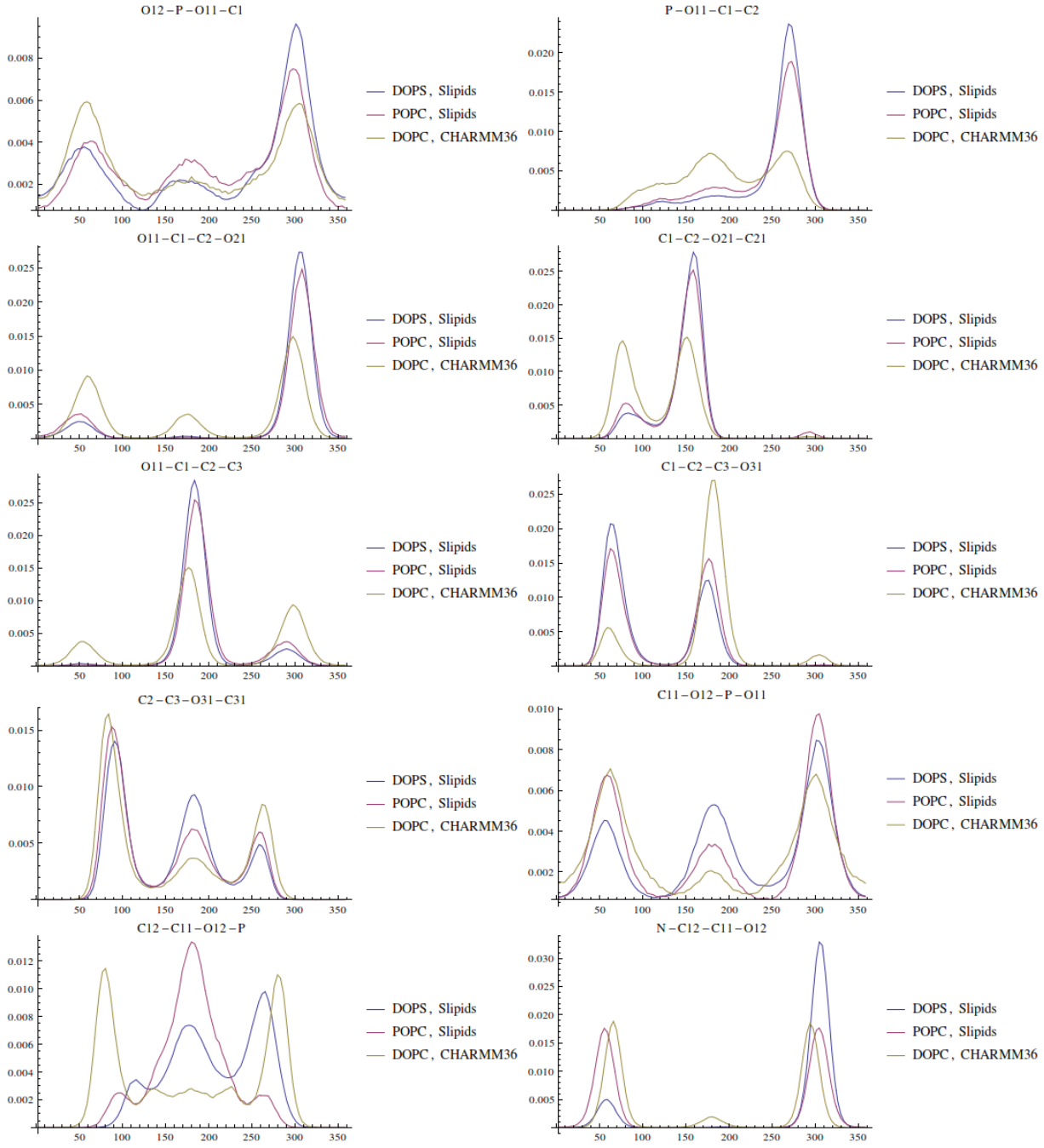

FIG. 13: Experimental results for sign measurement for POPS sample

[35] O. S. Ollila and G. Pabst, Biochimica et Biophysica Acta (BBA) - Biomembranes **1858**, 2512 (2016).

[36] F. Borle and J. Seelig, Chemistry and Physics of Lipids **36**, 263 (1985).

[37] P. M. Macdonald and J. Seelig, Biochemistry **26**, 1231 (1987).

[38] P. G. Scherer and J. Seelig, Biochemistry **28**, 7720 (1989).

[39] H. Akutsu and J. Seelig, Biochemistry **20**, 7366 (1981).

ToDo